Biochemistry and Biophysics Reports 20 (2019) 100678

Contents lists available at ScienceDirect

Biochemistry and Biophysics Reports

journal homepage: www.elsevier.com/locate/bbrep

# Antifibrotic effect of methylated quercetin derivatives on TGFβ-induced hepatic stellate cells

Munkhzul Ganbold[a], Yasuhiro Shimamoto[b], Farhana Ferdousi[c], Kenichi Tominaga[b], Hiroko Isoda[a,b,c,d,*]

[a] School of Integrative and Global Majors (SIGMA), University of Tsukuba, 1-1-1 Tennodai, Tsukuba, Ibaraki, 305-8572, Japan
[b] Interdisciplinary Research Center for Catalytic Chemistry, National Institute of Advanced Industrial Science and Technology (AIST), AIST Tsukuba Central 5-2, Tsukuba, Ibaraki, 305-8565, Japan
[c] Alliance for Research on the Mediterranean and North Africa (ARENA), University of Tsukuba, 1-1-1 Tennodai, Tsukuba, Ibaraki, 305-8572, Japan
[d] Life and Environmental Sciences, University of Tsukuba, Japan1-1-1 Tennodai, Tsukuba, Ibaraki, 305-8572, Japan

ARTICLE INFO

*Keywords:*
Quercetin
Isorhamnetin
Azaleatin
3-O-Methylquercetin
Tamarixetin
Rhamnetin
Fibrosis
Hepatic stellate cells

ABSTRACT

Quercetin (QCT) and isorhamnetin (ISO), natural flavonoids, were both shown to possess antifibrotic activity in *in vivo* and *in vitro* models of hepatic fibrosis. Although ISO is a direct metabolite of QCT differing by a methyl group, it has been reported to be absorbed more adequately and eliminated slower than QCT after oral administration. Our aim of the study was to investigate biological effect of mono-methylated QCT derivatives against fibrosis using rat hepatic stellate cells (HSC-T6). All test derivatives were synthesized from QCT. HSC-T6 cells were induced by TGFβ and treated with derivatives followed by cell proliferation assay, immunofluorescence staining of αSMA, and gene expression analysis of fibrosis markers. All compounds showed a dose- and time-dependent antiproliferation effect. ISO, 3-O-methylquercetin (3MQ), and rhamnetin (RHA) reduced αSMA mRNA; 3MQ prevented the augmentation of collagen I mRNA; and compounds, except azaleatin and 3MQ, reduced Timp1 mRNA expression in TGFβ-induced HSCs. In conclusion, each compound had singular effect against different features of fibrosis depending on the position of methyl group although the further mechanism of action of compounds during fibrosis development remains to be investigated. These findings suggest that antifibrotic effect of quercetin can be enhanced by adding methyl group on functionally important position.

## 1. Introduction

Liver fibrosis is a hepatic chronic disease characterized by the excessive accumulation of extracellular matrix (ECM) which can progress to irreversible scarring and end-stage liver diseases if the injury is persistent and chronic. However, hepatic fibrosis is orchestrated primarily by the hepatic stellate cells (HSC), a pleiotropic cell comprising one-third of the nonparenchymal cells and 5% of the total hepatic cells in normal human liver and residing in the perisinusoidal space of Disse. Chronic hepatic injury caused by various viral infections, metabolic disorders, alcoholism, and nonalcoholic steatohepatitis (NASH) leads to activation of HSCs from quiescent state into proliferative, migratory, and contractile myofibroblasts to produce ECM molecules such as collagen resulting in fibrosis, scarring, and subsequent liver damage [1–3].

Flavonoids are natural polyphenols widely presented in vegetables, fruits, seeds, and stems. They have been considered as one of the most important beneficial agents against cancers, cardiovascular, and neurodegenerative disorders [4]. Recent researches have demonstrated that the bioactive forms of flavonoids are the conjugates and metabolites that arise from their natural aglycone forms on absorption. Quercetin (QCT) is one of the most extensively studied flavonols that possesses strong anticancer, anti-inflammatory, antioxidant, antifibrogenic, and as well as cardio- and neuroprotective effects. However, QCT is generally not present in aglycone form in the plasma and occurs only in conjugated forms [5]. Generally, 20–40% of QCT is methylated in the 3′-position, yielding isorhamnetin (ISO). ISO is also found as a natural flavonoid in several plants and plant-derived foods, and shown to inhibit proliferation of breast cancer cells, protect HepG2 cells against oxidative stress, and attenuate inflammatory bowel disease [6,7]. Recent studies also showed its antioxidant, anti-obesity, and antifibrotic effects in rodents [8–10]. ISO has been shown not only to have similar biological effect *in vivo* and *in vitro* studies but also to be

* Corresponding author. Faculty of Life and Environmental Sciences, University of Tsukuba, 1-1-1 Tennodai, Tsukuba, Ibaraki, 305-8572, Japan.
*E-mail address:* isoda.hiroko.ga@u.tsukuba.ac.jp (H. Isoda).

https://doi.org/10.1016/j.bbrep.2019.100678
Received 3 July 2019; Received in revised form 2 August 2019; Accepted 10 August 2019
Available online 16 August 2019

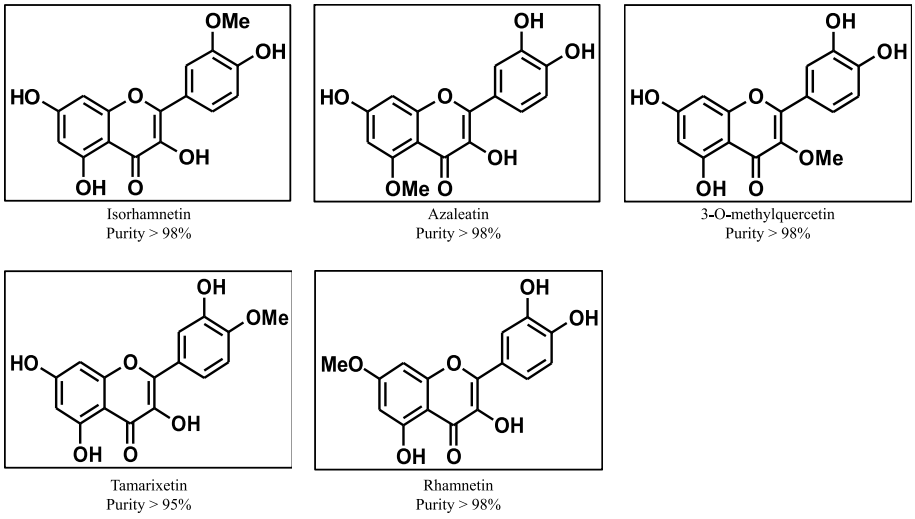


**Fig. 1.** Chemical structure and purity of synthesized compounds.

absorbed more adequately and eliminated slowly than its unmethylated parent – QCT [11].

Thus, in the present study, we synthesized several monomethylated quercetin derivatives, namely, ISO, 3-*O*-methyl quercetin (3MQ), azaleatin (AZA), rhamnetin (RHA) and tamarixetin (TAM), and investigated their antifibrotic effect on the activation and proliferation of HSCs and on the production of ECM using transforming growth factor-β (TGFβ)-induced HSC-T6 cells to answer whether the addition of methyl group improves the biological activity of quercetin against fibrogenesis.

## 2. Materials and methods

### 2.1. NMR data of methylated quercetin

Five different mono-methylated QCT derivatives: ISO, AZA, 3MQ, TAM, and RHA were synthesized from commercially available QCT (Fujifilm Wako Pure Chemical Corp., Tokyo, Japan) in reference to reported paper [12]. All synthesized methylquercetin was in good agreement with reported data [13–16]. Chemical structure and purity of each compound were shown in Fig. 1.

Isorhamnetin: yellow solid.; $^{1}$H NMR (400 MHz, DMSO-d6) δ = 7.73 (d, *J* = 2Hz, 1H), 7.67 (dd, *J* = 8.2, 2.2 Hz, 1H), 6.93 (d, *J* = 8.2 Hz, 1H), 6.46 (d, *J* = 2.2 Hz, 1H), 6.18 (d, *J* = 2.2 Hz, 1H), 3.83 (s, 3H); $^{13}$C NMR NMR (100 MHz, DMSO) δ = 175.9, 164.0, 160.7, 156.2, 148.8, 147.4, 146.6, 135.8, 122.0, 121.7, 115.6, 111.7, 103.0, 98.2, 93.6, 55.8.

Azaleatin: yellow solid.; $^{1}$H NMR (400 MHz, MeOD) δ = 7.70 (d, *J* = 2.8 Hz, 1H), 7.60 (dd, *J* = 8.8, 2.8 Hz, 1H), 6.87 (d, *J* = 2.2 Hz, 1H), 6.49 (d, *J* = 2.0 Hz, 1H), 6.38 (d, *J* = 2.0 Hz, 1H), 3.91 (s, 3H); $^{13}$C NMR NMR (100 MHz, MeOD) δ = 173.7, 164.7, 162.2, 160.1, 148.5, 146.3, 144.8, 138.7, 124.2, 121.3, 116.3, 115.7, 106.4, 96.8, 95.9, 56.5.

3-O-Methylqurcetin: yellow solid.; $^{1}$H NMR (400 MHz, MeOD) δ = 7.59 (d, *J* = 2.8 Hz, 1H), 7.50 (dd, *J* = 8.8, 2.8 Hz, 1H), 6.88 (d, *J* = 8.8 Hz, 1H), 6.35 (d, *J* = 2.0 Hz, 1H), 6.16 (d, *J* = 2.0 Hz, 1H), 3.76 (s, 3H); $^{13}$C NMR NMR (100 MHz, MeOD) δ = 178.7, 164.5, 161.8, 157.1.156.7, 148.6, 145.2, 138.2, 121.7, 121.0, 115.2, 115.1, 104.6, 98.5, 93.4, 59.2.

Tamarixetin: yellow solid.; $^{1}$H NMR (400 MHz, MeOD) δ = 7.76–7.73 (m, 2H), 7.05 (d, *J* = 8.8 Hz, 1H), 6.39 (d, *J* = 2.4 Hz, 1H), 6.18 (d, *J* = 2.4 Hz, 1H), 3.93 (s, 3H).

Rhamnetin: yellow solid.; $^{1}$H NMR (400 MHz, MeOD) δ = 7.76 (d, *J* = 2.4 Hz, 1H), 7.66 (dd, *J* = 8.8, 2.0 Hz, 1H), 6.88 (d, *J* = 8.8 Hz, 1H), 6.58 (d, *J* = 2.4 Hz, 1H), 6.31 (d, *J* = 2.4 Hz, 1H), 3.89 (s, 3H).

### 2.2. Chemicals and reagents

A stock solution of 100 mM for each compound was prepared by dissolving in DMSO and stored at −20 °C until use. Working solution (treatment) was prepared before use by diluting the stock solution in the culture media. Thus, the final concentration of DMSO in the medium did not exceed 0.04% for 40 μM, and 0.02% for 20 μM of treatment. Human recombinant TGFβ was purchased from Peprotech (NJ 08553, USA), reconstituted according to the manufacturer's instruction, and stored at −20 °C until use. Anti-collagen I (ab34710), anti-alpha smooth muscle actin (ab5694), AlexaFluor 488 labeled donkey anti-rabbit (ab150073) antibodies were purchased from Abcam (Tokyo, Japan). ProLong Diamond antifade mountant with 4′,6-Diamidino-2-Phenylindole (DAPI: double stranded DNA staining) was purchased from Invitrogen (ThermoFisher, USA).

### 2.3. Cell line and culture condition

Rat hepatic stellate cell (HSC-T6) line was purchased from Millipore (Millipore, CA, USA). As recommended by Millipore, cells were routinely cultured in DMEM-High glucose (D5796, Sigma-Aldrich, USA) containing 2.5 mM L-Glutamine supplemented with 10% FBS (Gibco, USA) and 1% penicillin (5000 μg/ml) – streptomycin (5000 IU/ml) (Lonza, Japan) at 37 °C in 5% $CO_2$ humidified incubator, and sub-cultured when the cells are approximately 90% confluent. Cells between passage 3 and 8 were used for further analysis.

### 2.4. Cell proliferation assay

HSC-T6 cells were seeded at a density of $1 \times 10^5$ cells/ml in a 96-well plate. After overnight incubation cells were treated with various concentrations of the compound for 12 and 24 h. 3-(4,5-dimethylthiazol-2-yl)-2,5-diphenyltetrazolium bromide (MTT) solution for final concentration of 0.5 mg/ml was added to the culture medium and incubated for 6h. After discarding the medium formazan crystals were dissolved in 10% sodium dodecyl sulfate (SDS) solution for overnight incubation. Absorbance at 570 nm was measured using microplate reader (Varioskan LUX), and the cell proliferation was calculated as Cell proliferation (%) = [(mean OD value of treated well – mean OD value of the blank) × 100%]/(mean OD value of untreated well – mean OD value of the blank). The experiment with six repeats in each concentration was replicated at least three times.

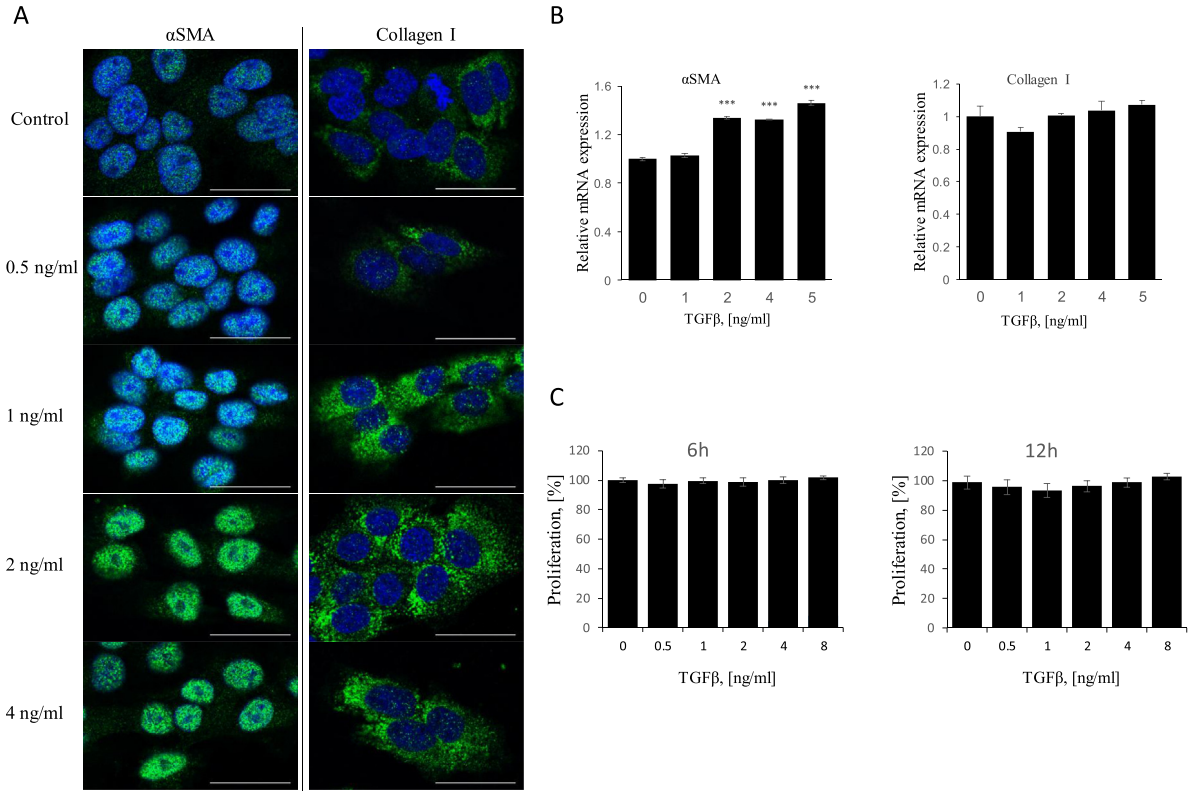


**Fig. 2.** TGFβ induced fibrosis in HSCs. (A) Immunodetection of αSMA and Collagen I in TGFβ-induced HSCs. Cells were incubated with different concentration of TGFβ for 24h; and αSMA (green, 1st column), collagen I (green, 2nd column) and nucleus (blue) were detected by immunofluorescence staining (Scale bar = 30 μm). Control represents non-treated negative control. (B) Gene expression of αSMA (*Acta2* gene) and Collagen I (*Col1a1* gene) in TGFβ-induced HSCs. Cells were incubated with different concentration of TGFβ for 24 h and qPCR analysis was performed. Data are shown as mean ± SEM of at least three independent experiments with significance ***$p < 0.001$ vs. non-treated control. (C) Effect of TGFβ on proliferation of HSCs. Cells were incubated with different concentration of TGFβ for 6 and 12 h, and cell proliferation rate was determined by MTT assay. Data are shown as mean ± SD of at least three independent experiments.

### *2.5. Immunofluorescence analysis*

HSC-T6 cells were seeded on cover slip at a density of $5 \times 10^4$ cells/ml in 6-well plate and incubated overnight to attach the surface. Cells were treated with 2 ng/ml of TGFβ to induce fibrosis in the presence or absence of compound. After 24 h of co-treatment, cells were washed twice with cold phosphate buffered saline (PBS) and fixed with 3.7% paraformaldehyde for 20 min at room temperature followed by rehydration with PBS and incubated in blocking solution containing 1% bovine serum albumin (BSA) and 0.1% Tween20 for 2 h. The slides were incubated with the primary antibody anti-collagen I at 1/100 dilution and anti-αSMA at 1/100 dilution for overnight at 4 °C. Consequently, the slides were incubated for 1 h with secondary antibody at 1/250 dilution after washing with PBS three times. The slides were mounted using ProLong Diamond with DAPI and observed under a Leica TCS SP8 confocal microscope.

### *2.6. Real-time reverse transcription polymerase chain reaction (RT-PCR) analysis*

HSC-T6 cells were seeded in 6-well plate at a density of $1 \times 10^5$ cells/ml and incubated overnight to attach the surface. Cells were treated with 2 ng/ml of TGFβ to induce fibrosis in the presence or absence of compound for 1h. Total RNA was extracted using ISOGEN reagent (Nippon Gene, Toyama, Japan) according to the manufacturer's instruction. First-strand cDNA was amplified from the total RNA (100 ng) using SuperScript III Reverse Transcriptase kit (Invitrogen, Carlsbad, CA, USA). The quantification of total RNA and cDNA was measured on NanoDrop 2000 spectrophotometer (Thermo Scientific, Wilmington, DE, USA). Real-time quantitative PCR of target gene expression was assayed by TaqMan predesigned primers (Applied Biosystems, Foster City, CA, USA) and TaqMan Gene Expression Master Mix (Life Technologies, Carlsbad, USA) using the 7500 Fast Real-Time PCR System (Applied Biosystems, Foster City, CA, USA). Collagen type 1 alpha 1 (Col1a1) (Rn01463848_m1), alpha smooth muscle actin (Acta2) (Rn01759928_g1), tissue inhibitor metalloproteinase-1 (Timp1) (Rn01430873_g1) and glyceraldehyde-3-phosphate dehydrogenase (Gapdh) (Rn01775763_g1) primers were purchased from Applied Biosystems. The $2^{-\Delta\Delta Ct}$ method was applied to calculate the relative mRNA expression levels using Gapdh as a housekeeping endogenous control.

### *2.7. Statistics*

All data are expressed as the mean ± standard error of the mean (SEM) unless otherwise indicated. Two-tailed Student's *t*-test was applied to assess the statistical significance of difference among the treatments. We conducted ANOVA followed by Dunnett's post-hoc test for multiple comparison among controls (NC and PC) and derivative-treated groups using IBM SPSS Statistics version 24.0. All graphs were prepared using Microsoft Excel 365. A value of $p < 0.05$ was considered as significant for all results.

## 3. Results

### *3.1. Optimization of TGFβ-induced HSC-T6 as a fibrosis cell model*

HSC activation plays a major role in hepatic fibrogenesis. In response to liver injury resulting from drugs, toxins, viral infection, and hepatic chronic diseases such as nonalcoholic steatohepatitis (NASH),

the production of profibrotic cytokines such as TGFβ is increased and triggers several intracellular signaling pathways leading to the activation of HSC. Upon their activation, HSCs undergo phenotypic modulation becoming motile, proliferative, and fibroblast-like, and increase αSMA secretion which promotes excessive deposition of ECM. In our preliminary study to determine the optimum concentration of TGFβ on the induction of fibrosis *in vitro*, HSC-T6 cells were treated with 0.5, 1, 2, 4 ng/ml of TGFβ for 24 h, and collagen I and αSMA were detected by immunofluorescence (Fig. 2A). Level of αSMA was slightly increased in HSC-T6 treated with 0.5 ng/ml TGFβ and remarkably increased in HSC-T6 treated with 2–4 ng/ml TGFβ. However, no visible difference was observed among treatments with 2 and 4 ng/ml of TGFβ (Fig. 2A, 1st column). Collagen I was significantly deposited after 24 h of treatment with 0.5 ng/ml of TGFβ compared with non-treated control and invariably increased with augmentation of dose until 4 ng/ml (Fig. 2A, 2nd column). Gene expression levels of collagen I and αSMA were measured after 24 h of treatment with TGFβ (Fig. 2B). Significant augmentation of αSMA gene expression reached from 2 ng/ml of TGFβ treatment, and stably increased with a higher dose of TGFβ induction. Gene expression of collagen I slightly increased with the augmentation of treatment dose but statistically not significant within the range of TGFβ concentration. We also examined the proliferation effect of TGFβ on HSC-T6. The proliferation rate of HSC-T6 compared to that of in non-treated control was not noticeably affected after the treatment with TGFβ from 0.5 to 8 ng/ml for 6 and 12 h (Fig. 2C). Therefore, we chose the dose of 2 ng/ml TGFβ, an adequate concentration to stimulate fibrosis markers without affecting the proliferation of HSC-T6, for further analysis.

### 3.2. Antiproliferation effect of derivatives on TGFβ-induced hepatic stellate cells

Upon activation, HSCs undergo proliferation which leads to aberrant production of ECM. Thus, to investigate the effect of test compounds on the proliferation of HSC-T6, we treated cells with 5, 10, 20, 40, 80 μM of the compound for 6, 12, and 24 h, and determined the cell viability (Fig. 3). However, after 6 h of treatment, all compounds, but not ISO, tend to increase the proliferation rate of HSC-T6 in a dose-dependent manner (Fig. 3A). After 12 h of treatment, proliferation was decreased in all compound treated HSC-T6 to the level comparable to NC. ISO effectively inhibited the proliferation from 40 μM of concentration (Fig. 3B). The incubation with 80 μM of the compound for 24 h markedly suppressed the proliferation of HSC-T6 (Fig. 3C). ISO, QCT, and 3MQ had inhibitory effect from 10 μM, and it was dose and time-dependent manner. AZA, RHA, and TAM inhibited the proliferation at 80 μM, however, their effect was not visible in a lower dose up to 12 h. Thus, we used 20 and 40 μM concentration for further analysis.

### 3.3. Effect of derivatives on TGFβ-induced production of αSMA and collagen I

To further discover the effect of compounds on TGFβ-induced production of αSMA, we treated TGFβ-induced HSC-T6 with 20 and 40 μM of the compound. After 24 h of incubation, αSMA was detected by immunofluorescence staining (Fig. 4A). We observed visibly decreased accumulation of αSMA in all compound-treated HSC-T6 compared to the positive control (PC). However, among test compounds, QCT, ISO, 3MQ, and RHA decreased αSMA at 20 μM, and inhibited more effectively at 40 μM showing their effect was dose-dependent. Inhibition effects of AZA and TAM were weaker compared to other derivatives, even though αSMA level was markedly decreased comparing to PC. Collagen I was also detected by immunofluorescence after 24 h of treatment in TGFβ-induced HSC-T6 to analyze the inhibitory effect of compounds (Fig. 4A). AZA, 3MQ, and TAM-treated cells showed effective inhibition of collagen I production, while partly inhibited in ISO-treated cells. QCT and RHA treatment slightly reduced the collagen presence compared to PC.

### 3.4. Effect of derivatives on TGFβ-induced fibrogenic gene expression

After finding that test compounds could significantly inhibit the production of αSMA at 20 μM of concentration after 24 h of treatment in TGFβ-induced HSC-T6, we chose to use this dose to determine their effect on the gene expression of collagen I, αSMA, and Timp1. As shown in Figs. 4B and 1 h of TGFβ treatment was enough to significantly increase the mRNA level of αSMA. Once co-treated with compounds, QCT, ISO and RHA inhibited this augmentation of the αSMA level. But AZA, 3MQ, and TAM treatment did not show inhibitory effect. When treated for 6 h, the expression level of αSMA was lower than the negative control (NC) in ISO and 3MQ-treated cells. However, the expression level of αSMA in AZA-treated cells tended to be decreased after 6 h of treatment, still remained higher than NC. On the other hand, both TAM and QCT showed significantly increased expression of αSMA after 6 h of treatment compared to that of NC. Collagen I mRNA was increased after 1 h of treatment but decreased after 6 h of treatment in those treated with QCT, AZA, 3MQ, and RHA time-dependently (Fig. 4B). Interestingly, after 6 h of 3MQ treatment, collagen I expression was drastically decreased to the level of NC. In ISO and TAM-treated cells collagen I mRNA level remained elevated. In addition, treatment with TGFβ for 6 h significantly increased the expression of Timp1 as shown in Fig. 4B. The increase of Timp1 mRNA was attenuated in cells treated with QCT, ISO, TAM, and RHA. In contrast, AZA and 3MQ were not able to inhibit the expression of Timp1 mRNA level.

## 4. Discussion

In the present study, we showed that methylquercetin derivatives depending on the methyl group position have different effects on proliferation and production of profibrotic gene expression in TGFβ-induced HSC-T6. It was also demonstrated that the optimum dose and time of incubation with TGFβ to stimulate fibrosis *in vitro* is an important experimental parameter to study the effect of compounds adequately.

Even though novel pathways and cellular signaling are being discovered to be involved in the development of liver fibrosis, TGFβ-induced pathways remain as the central target in therapeutic strategy [17,18]. Chronically increased TGFβ in response to a liver injury activates HSC-T6, in turn, HSC-T6 are the main driver in the fibrogenic process undergoing phenotypic modification from quiescent to activated state which leads to increased proliferation, and excessive production of ECM. Among various therapeutic strategies retardation of HSCs activation and proliferation, and degradation of ECM are more promising approaches in the resolution of fibrosis [19,20]. However, direct targeting of TGFβ may result later in undesirable controversial cellular response because it is a pleiotropic cytokine involved virtually in all stage of liver physiologic and pathologic process [21]. Thus, a molecular agent which can regulate TGFβ-induced fibrogenic pathways has more clinical implication.

Accumulating data have shown that natural flavonoids and herbal extracts have the potential to prevent and regress liver fibrosis through their antioxidant activity [10,22,23]. Yang et al. revealed that ISO treatment reduced pathologic features in $CCl_4$-induced liver fibrosis, and level of phosphorylated Smad2/3 in primary HSCs and LX-2 (human activated HSC line) via inhibition of TGFβ/Smad pathway [10]. Li et al. also showed that ISO remarkably inhibits A549 lung cancer cells growth by inducing apoptotic changes [24]. Our results demonstrated that ISO and 3MQ had stronger inhibition effect on the proliferation of HSC-T6 followed by decreased αSMA and Timp1 mRNA level after TGFβ-induction. Moreover, the methyl groups in ISO and 3MQ are spatially located closer than other derivatives suggesting methyl groups on C-3' and C-3 position may have functional role to exert biological activity of these derivatives.

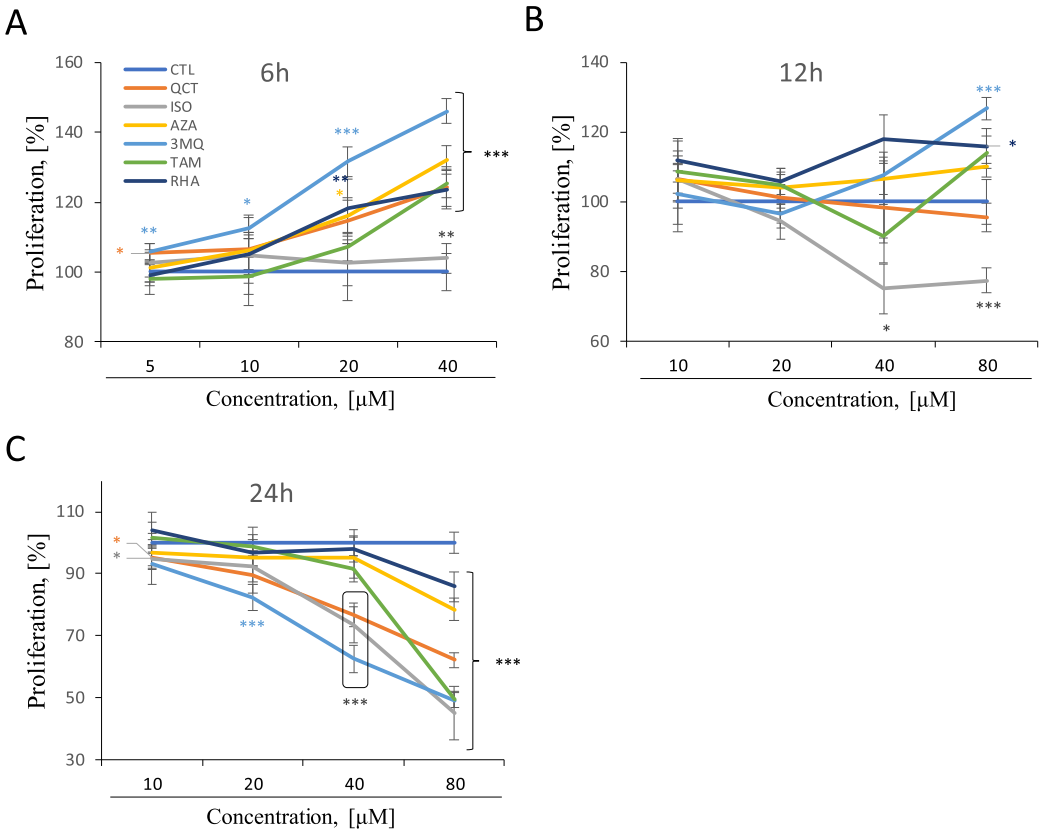


**Fig. 3.** Inhibitory effect of compounds on proliferation of HSC-T6. Cells were incubated with different concentration of compound for 6 h (A), 12 h (B), and 24 h (C); and cell viability was measured by MTT assay. Data are shown as mean ± SD of at least three independent experiments with significance *p < 0.05, **p < 0.01 and ***p < 0.001 vs. non-treated control (CTL).

Kawada and colleagues demonstrated that QCT prevents the activation of cultured HSC-T6 by suppressing the expression of αSMA and dose-dependently inhibits the serum-dependent proliferation [22]. Moreover, Wu et al. showed that liver fibrosis induced by bile duct ligation and $CCl_4$-injection was prevented in QCT-treated mice by inhibition of HSCs activation and reduction of autophagy [25]. In our results, QCT treatment could slightly reduce collagen I and Timp1 gene expression, but not αSMA expression, after 6 h of incubation with TGFβ. Our finding supports previously reported results of the inhibitory effect of QCT on HSCs proliferation. The effect of AZA and TAM on inhibition of αSMA and collagen I mRNA was not effective compared to PC. It indicates that the hydroxyl group in at least C-5 and C-4' position is necessary to exert their biological activity, otherwise methylation on those positions caused their loss of activity. Even though the mechanism of action of each compound, and their effect *in vivo* remained to be elucidated for further drug development, taken together, our data demonstrated that mono-methylated derivatives possess different biological activity than quercetin, and the antifibrotic effect of quercetin can be pharmacologically improved by adding methyl group on functionally important position.

## Acknowledgments

This research was partially funded by the Japan Science and Technology Agency (JST) and the Japan International Cooperation Agency (JICA) Science and Technology Research Partnership for Sustainable Development (SATREPS): JPMJSA1506, and JST-Center of Innovation (COI) project; and Mongolian-Japan Engineering Education Development Project (MJEED).

## List of abbreviation

| | |
|---|---|
| 3MQ | 3-O-methylquercetin |
| ACTA2 | Actin alpha 2 gene |
| AZA | Azaleatin |
| COL1A1 | Type I collagen gene |
| DAPI | 4′,6-Diamidino-2-Phenylindole |
| DMEM | Dulbecco's modified eagle medium |
| DMSO | Dimethyl sulfoxide |
| ECM | Extracellular matrix |
| FBS | Fetal bovine serum |
| HSCs | Hepatic stellate cells |
| HSC-T6 | Rat hepatic stellate cell line |
| ISO | Isorhamnetin |
| NASH | Nonalcoholic steatohepatitis |
| NC | Negative control |
| NMR | Nuclear magnetic resonance |
| PBS | Phosphate buffered saline |
| PC | Positive control |
| QCT | Quercetin |
| RHA | Rhamnetin |
| SDS | Sodium dodecyl sulfate |
| SEM | standard error of mean |
| TAM | Tamarixetin |
| TGFβ | Transforming growth factor beta 1 |
| TIMP1 | Tissue inhibitor of metalloproteinase 1 gene |
| αSMA | Alpha smooth muscle actin |

## Transparency document

Transparency document related to this article can be found online at

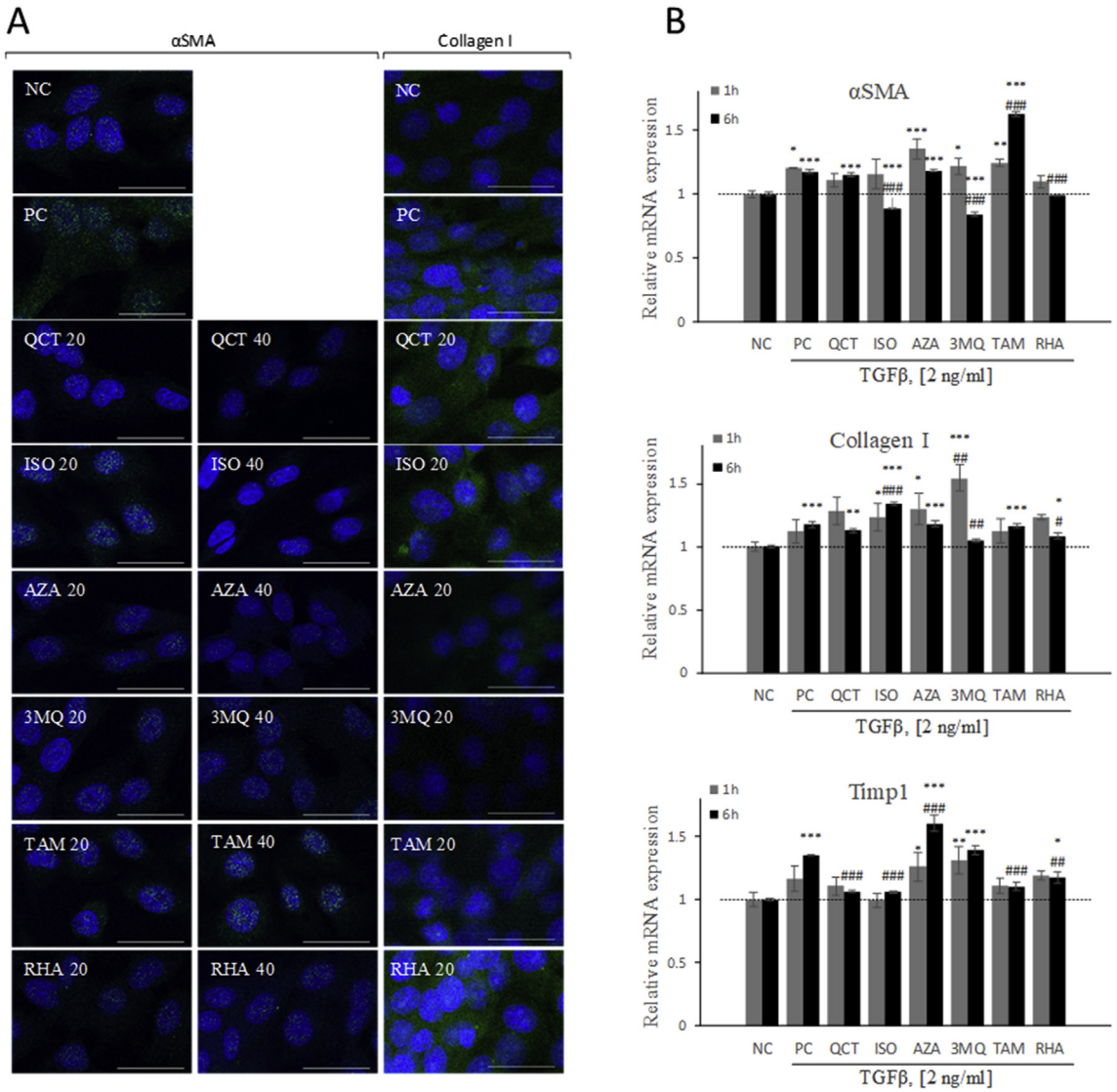


**Fig. 4.** Inhibitory effect of compounds on expression of fibrogenic markers in TGFβ-induced HSCs. (A) Cells were incubated with 20 and 40 μM concentration of compound in the presence of 2 ng/ml of TGFβ for 24 h, and αSMA (green) or Collagen I (green) and nucleus (blue) were detected by immunofluorescence staining (Scale bar = 30 μm). NC – non treated negative control, PC – treated with 2 ng/ml of TGFβ positive control. (B) Cells were treated with 2 ng/ml of TGFβ and 20 μM of compound for 1 and 6 h, and mRNA level of αSMA, Collagen I, and Timp1 were determined by real time qPCR. Data are shown as mean ± SEM of at least three repetitions with significance *p < 0.05, **p < 0.01 and ***p < 0.001 vs. non-treated, non-induced control (NC); and #p < 0.05, ##p < 0.01 and ###p < 0.001 vs. TGFβ -induced positive control (PC) by ANOVA followed by Dunnett's post-hoc test. Horizontal dash line shows the level of NC.

https://doi.org/10.1016/j.bbrep.2019.100678

## References


[1] T. Higashi, S.L. Friedman, Y. Hoshida, Hepatic stellate cells as key target in liver fibrosis, Adv. Drug Deliv. Rev. 121 (2017) 27–42, https://doi.org/10.1016/j.addr.2017.05.007.

[2] J.E. Puche, Y. Saiman, S.L. Friedman, Hepatic stellate cells and liver fibrosis, Comp. Physiol. 3 (2013) 1473–1492, https://doi.org/10.1002/cphy.c120035.

[3] C.Y. Zhang, W.G. Yuan, P. He, J.H. Lei, C.X. Wang, Liver fibrosis and hepatic stellate cells: etiology, pathological hallmarks and therapeutic targets, World J. Gastroenterol. 22 (2016) 10512–10522, https://doi.org/10.3748/wjg.v22.i48.10512.

[4] C. Manach, A. Scalbert, C. Morand, C. Rémésy, L. Jiménez, Polyphenols : food sources and bioavailability, Am. J. Clin. Nutr. 79 (2004) 727–747, https://doi.org/10.1093/ajcn/79.5.727.

[5] J.P.E. Spencer, G.G.C. Kuhnle, R.J. Williams, C. Rice-Evans, Intracellular metabolism and bioactivity of quercetin and its in vivo metabolites, Biochem. J. 372 (2003) 173–181, https://doi.org/10.1042/bj20021972.

[6] J.H. Yang, B.Y. Shin, J.Y. Han, M.G. Kim, J.E. Wi, Y.W. Kim, I.J. Cho, S.C. Kim, S.M. Shin, S.H. Ki, Isorhamnetin protects against oxidative stress by activating Nrf2 and inducing the expression of its target genes, Toxicol. Appl. Pharmacol. 274 (2014) 293–301, https://doi.org/10.1016/j.taap.2013.10.026.

[7] S. Hu, L. Huang, L. Meng, H. Sun, W. Zhang, Y. Xu, Isorhamnetin inhibits cell proliferation and induces apoptosis in breast cancer via Akt and mitogen-activated protein kinase kinase signaling pathways, Mol. Med. Rep. 12 (2015) 6745–6751, https://doi.org/10.3892/mmr.2015.4269.

[8] F. Zar Kalai, J. Han, R. Ksouri, A. El Omri, C. Abdelly, H. Isoda, Antiobesity effects of an edible halophyte Nitraria retusa Forssk in 3T3-L1 preadipocyte differentiation and in C57B6J/L mice fed a high fat diet-induced obesity, Evidence-Based Complement, Altern. Med. 2013 (2013) 368658, https://doi.org/10.1155/2013/368658.

[9] F. Zar Kalai, J. Han, R. Ksouri, C. Abdelly, H. Isoda, Oral administration of Nitraria retusa ethanolic extract enhances hepatic lipid metabolism in db/db mice model "BKS.Cg-Dock7m+/+ Leprdb/J" through the modulation of lipogenesis-lipolysis balance, Food Chem. Toxicol. 72 (2014) 247–256, https://doi.org/10.1016/j.fct.2014.07.029.

[10] J.H. Yang, S.C. Kim, K.M. Kim, C.H. Jang, S.S. Cho, S.J. Kim, S.K. Ku, I.J. Cho, S.H. Ki, Isorhamnetin attenuates liver fibrosis by inhibiting TGF-β/Smad signaling and relieving oxidative stress, Eur. J. Pharmacol. 783 (2016) 92–102, https://doi.org/10.1016/j.ejphar.2016.04.042.

[11] G. Li, X. Zeng, Y. Xie, Z. Cai, J.C. Moore, X. Yuan, Z. Cheng, G. Ji, Pharmacokinetic properties of isorhamnetin, kaempferol and quercetin after oral gavage of total flavones of Hippophae rhamnoides L. in rats using a UPLC-MS method, Fitoterapia 83 (2012) 182–191, https://doi.org/10.1016/j.fitote.2011.10.012.

[12] Z.H. Shi, N.G. Li, Y.P. Tang, Wei-Li, Lian-Yin, J.P. Yang, Hao-Tang, J.A. Duan, Metabolism-based synthesis, biologic evaluation and SARs analysis of O-methylated

analogs of quercetin as thrombin inhibitors, Eur. J. Med. Chem. 54 (2012) 210–222, https://doi.org/10.1016/j.ejmech.2012.04.044.
[13] S. Parveen, N. Riaz, M. Saleem, J. Khan, S. Ahmad, M. Ashraf, S.A. Ejaz, R.B. Tareen, A. Jabbar, Bioactive phenolics from launaea intybacea, J. Chem. Soc. Pak. 34 (2012) 1513–1519.
[14] S.A. Villaume, J. Fu, I. N'Go, H. Liang, H. Lou, L. Kremer, W. Pan, S.P. Vincent, Natural and synthetic flavonoids as potent Mycobacterium tuberculosis UGM inhibitors, Chem. Eur J. 23 (2017) 10423–10429, https://doi.org/10.1002/chem.201701812.
[15] K. Yamauchi, T. Mitsunaga, M. Inagaki, T. Suzuki, Synthesized quercetin derivatives stimulate melanogenesis in B16 melanoma cells by influencing the expression of melanin biosynthesis proteins MITF and p38 MAPK, Bioorg. Med. Chem. 22 (2014) 3331–3340, https://doi.org/10.1016/j.bmc.2014.04.053.
[16] S.L. Guzmán-Gutiérrez, A. Nieto-Camacho, J.I. Castillo-Arellano, E. Huerta-Salazar, G. Hernández-Pasteur, M. Silva-Miranda, O.A. Ello-Nájera, O. Sepúlveda-Robles, C.I. Espitia, R. Reyes-Chilpa, Mexican propolis: a source of antioxidants and anti-inflammatory compounds, and isolation of a novel chalcone and ε-caprolactone derivative, Molecules 23 (2018) E334, https://doi.org/10.3390/molecules23020334.
[17] A.M. Gressner, R. Weiskirchen, K. Breitkopf, S. Dooley, Roles of TGF-beta in hepatic fibrosis, Clin. Chem. 7 (2002) d793–807.
[18] B. Piersma, R.A. Bank, M. Boersema, Signaling in fibrosis: TGF-β, WNT, and YAP/TAZ converge, Front. Med. 2 (2015) 1–14, https://doi.org/10.3389/fmed.2015.00059.
[19] F. Xu, D. Zhou, X. Meng, X. Wang, C. Liu, C. Huang, J. Li, L. Zhang, Smad2 increases the apoptosis of activated human hepatic stellate cells induced by TRAIL, Int. Immunopharmacol. 32 (2016) 76–86, https://doi.org/10.1016/j.intimp.2016.01.013.
[20] D. Ezhilarasan, E. Sokal, M. Najimi, Hepatic fibrosis: it is time to go with hepatic stellate cell-specific therapeutic targets, Hepatobiliary Pancreat. Dis. Int. 17 (2018) 192–197, https://doi.org/10.1016/j.hbpd.2018.04.003.
[21] I. Fabregat, J. Moreno-Càceres, A. Sánchez, S. Dooley, B. Dewidar, G. Giannelli, P. ten Dijke, TGF-β signalling and liver disease, FEBS J. 283 (2016) 2219–2232, https://doi.org/10.1111/febs.13665.
[22] N. Kawada, S. Seki, M. Inoue, T. Kuroki, Effect of antioxidants, resveratrol, quercetin, and N-acetylcysteine, on the functions of cultured rat hepatic stellate cells and kupffer cells, Hepatology 27 (1998) 1265–1274, https://doi.org/10.1002/hep.510270512.
[23] R. Jadeja, R.V. Devkar, S. Nammi, R. Jadeja, R.V. Devkar, S. Nammi, Herbal medicines for the treatment of nonalcoholic steatohepatitis: current scenario and future prospects, Evid. Based Complement Altern. Med. 2014 (2014) 648308, https://doi.org/10.1155/2014/648308.
[24] Q. Li, F.Q. Ren, C.L. Yang, L.M. Zhou, Y.Y. Liu, J. Xiao, L. Zhu, Z.G. Wang, Anti-proliferation effects of isorhamnetin on lung cancer cells in vitro and in vivo, Asian Pac. J. Cancer Prev. APJCP 16 (2015) 3035–3042, https://doi.org/10.7314/APJCP.2015.16.7.3035.
[25] L. Wu, Q. Zhang, W. Mo, J. Feng, S. Li, J. Li, T. Liu, S. Xu, W. Wang, X. Lu, Q. Yu, K. Chen, Y. Xia, J. Lu, L. Xu, Y. Zhou, X. Fan, C. Guo, Quercetin prevents hepatic fibrosis by inhibiting hepatic stellate cell activation and reducing autophagy via the TGF-β1/Smads and PI3K/Akt pathways, Sci. Rep. 7 (2017) 9289, https://doi.org/10.1038/s41598-017-09673-5.